Available online at www.sciencedirect.com
SCIENCE DIRECT®
Talanta 64 (2004) 750–757
Talanta
www.elsevier.com/locate/talanta

Microchip capillary electrophoresis with electrochemical detector for precolumn enzymatic analysis of glucose, creatinine, uric acid and ascorbic acid in urine and serum

Hui-Ling Lee, Show-Chuen Chen*

Department of Chemistry, Fu-Jen Catholic University, No. 510 Road Chang Cheng, Hsinchuang 242, Taipei, Taiwan, ROC

Received 19 February 2004; received in revised form 25 March 2004; accepted 26 March 2004
Available online 18 May 2004

Abstract

An integrated multiple-enzymatic assay was performed on a (microchip capillary electrophoresis) μCE–EC chip capable of precise intake of sample or reagents in nanoliters. Incorporating multiple-enzyme assay into the μCE chip is relatively new—rendering simultaneous analysis of creatinine and uric acid a snap.

Added to the list of merits in this study are the enhanced sensitivity down to 1 μM and a broader spectrum of analytes—inclusive of glucose for the long-time sufferers of diabetes. The performance was orchestrated to attain the claimed level: employing the end-channel electrode mode to tame the noises and the precolumn enzymatic reaction to stabilize the baseline. The 10 μm embedded Pt electrode, deposited at the end of the 30 μm wide separation channel, benefited chip fabrication besides noise reduction. The optimized conditions were 20 mM phosphate buffer (pH 7.5), +1.5 kV separation voltage and +1.0 V detection potential (versus Ag/AgCl). The migration time was repeatable within the deviation of 0.5% R.S.D. ($n = 7$), but the peak currents ranged from 1.5 to 2.2% R.S.D. The detection limits (S/N = 3) ranged from 0.71 μM for ascorbic acid to 10 μM for glucose. The calibration curve was linear from 10 to 800 μM ($R^2 > 0.995$). Glucose, creatinine, uric acid and ascorbic acid as model analytes, in pure form or in serum and urine samples, were tested to verify its feasibility.

Keywords: Microchip; Capillary electrophoresis (CE); Precolumn enzymatic analysis

1. Introduction

The micro total analysis systems (μ-TAS), rapidly grown over the last decade, had promised the advantages of small size, less reagents and the integrating power via annexing lab procedures. And we were marveled at the name of 'lab-on-a-chip' coined as if witness a utopia. But such architecture was too grand a scale even to attempt, which had left room for the simpler and immediately workable microchip capillary electrophoresis (μCE) [1–11]. Its advantages of custom design, waste reduction, speed and portability were obvious [3,4]. In particular, on-chip enzymatic assays had reached a certain level of success to combine the analytical powers of μCE devices with high specificity of enzyme reactions [5]. Ramsey and co-workers [6,7] described microchip separation devices for performing enzyme (galactose or acetylcholinesterase) inhibition assays with fluorescence detection. Zugel et al. [8] described microchip assays using leucine aminopeptidase (LAP). Wang [5] interfaced enzyme-based biochip assays with various amperometric detectors. Many instances indicated that electrochemical detection offered advantages for μCE, especially its compatibility with micromachining technologies, miniaturization of both the detector and control instrumentation, and superb sensitivity [9,10]. On-column enzyme reactions of glucose oxidase, alcohol dehydrogenase [11,12] and creatininase (CA), creatinase (CI), and sarcosine oxidase (SOx) [13] had all been employed for selective measurements of glucose, ethanol and creatinine. Postcolumn reactions were recently used to monitor amino acid and on-chip immunological reactions [14,15], but unsuitable for μCE–EC due to slow response.

Concentrations of creatinine, glucose, uric acid and ascorbic acid in biological fluid are important factors in the evaluation of renal, muscular, and diabetic function [16,17].

* Corresponding author. Tel.: +886-2-29031111/3575; fax: +886-2-29023209.
E-mail address: huiling.lee@msa.hinet.net (S.-C. Chen).

0039-9140/$ – see front matter © 2004 Elsevier B.V. All rights reserved.
doi:10.1016/j.talanta.2004.03.046

Creatinine as the final product of creatine metabolism in mammals serves to index the renal glomerular filtration rate [18]. Uric acid, as derived from purine breakdown, lends itself to diagnosing a range of disorders associated with purine metabolism—notably gout, hyperuricaemia and Lesch–Nyham syndrome [19]. The glucose level in blood indicates hyper- and hypoglycemia [20].

The need for a simple yet reliable and rapid method to monitor glucose, creatinine, uric acid and ascorbic acid had prompted the development of various enzyme-based biosensors [21], chromatographic [22,23], electrophoretic [24] methods. Most of the analytical methods developed for creatinine were based on spectrophotometric detection of Jaffe reaction [25], which, however, were prone to interferences from glucose, pyruvate, acetoacetate, bilirubin, and dopamine [17]. Multi-enzymatic analysis, proposed by Tsuchida and Yoda [21], employed creatininase, creatinase and sarcosine oxidase in sequence to convert creatinine to H_2O_2. Wang et al. [12] went further to develop microchip separation devices for simultaneous measurement of renal markers, namely creatinine and uric acid. In their study, sample and enzyme-reagent streams were mixed at the channel intersection, which posed a basic problem of sensitivity loss as a result of unstabilized background. The present study used the precolumn multiple-enzyme reactions with ample time to react before injection. It gave fast responding and reproducible peaks in spite of multiple mixing steps involved.

2. Experimental

2.1. Materials and reagents

Dopamine, catechol, creatinine, glucose, β-nicotinamide adenine dinucleotide (NADH), ascorbic acid, 2-(*N*-morpholino)-enthanesulfonic acid (MES), creatininase (100 U mg^{-1}, from Pseudomonas species), creatinase (8.6 U mg^{-1}, from Pseudomonas species) and sarcosine oxidase (47 U mg^{-1}, from Bacillus species) were obtained from Sigma (St. Louis, MO). Glucose dehydrogenase (GDH, 100 U mg^{-1}, from Bacillus megaterium) and uric acid were obtained from Fluka (Switzerland). All chemicals were used as received. The performance of the chip was checked by a running buffer of 25 mM MES adjusted to pH 6.5 [26] as shown in Fig. 2. Standard solutions of various concentrations were prepared by diluting 0.01 M stock solution, with the running buffer of 20 mM phosphate buffer adjusted to pH 7.5. All solutions were filtered with 0.45 μm membrane prior to use (Alltech, PA, USA).

2.2. Apparatus

A high-voltage power supply from Bertan 230-30R (Valhalla, NY, USA) adjustable from 0 to 30 kV was used for electrophoretic separation. Electrochemical detection was performed with Electrochemical Analyzer 812 (CH Instruments, Austin, TX, USA) connected to a Pentium 166 MHz computer (32 MB RAM).

A homemade glass microchip consisteing of reservoirs for reagent enzymes, sample, running buffer and sample waste is shown in Fig. 1A.

2.3. Microfabrication of the planar platinum electrodes

Photomask was done in National Nano Device Laboratories (Hsinchu, Taiwan). All electrodes were fabricated by the standard photolithographic techniques and the wet etching process [27]. Pyrex glass (Corning 7740, 500 μm thickness), obtained from I.G.S. (Sunnyvale, CA), was sonicated in acetone, and water, each for 10 min, then dipped in hot Piranha acid (H_2SO_4/H_2O_2, 3:1) for 10 min. (*Caution!* Piranha acid solution is a powerful oxidizing agent, which reacts violently with organic compounds. It should be handled with extreme care.) Chip cleansing was completed by dipping in $NH_4OH/H_2O_2/H_2O$ (1:1:2) for 10 min. After soaking in water, it was ready for electrode deposition by the lift-off technique [27]. The photoresist, S1813, was obtained from Shipley Company of Marlborough, MA.

Electrode deposition was initiated by depositing an adhesive layer of 35 nm titanium (titanium sheet 99%, Alfa Aesar, USA), then the 200 nm platinum layer (99.99%, Goodfellow Corp., Malvern, PA, USA) using an electron beam evaporator (LUAC, Japan) under a vacuum below 10^{-6} Torr. After deposition, it was sonicated in an acetone bath to remove the photoresist and unwanted metal.

2.4. Microchip fabrication

Photolithography was done at the MEMS Facility (National Taiwan University, NTU). The microfluidic network was patterned on an 18 mm × 58 mm × 0.5 mm thick Pyrex 7740 wafer using the standard photolithographic techniques. Pyrex glass was subjected to a series of cleaning baths in a clean room, each for 10 min: acetone and water in the sonic bath, then 120 °C Piranha acid solution (H_2SO_4/H_2O_2, 3:1) and $NH_4OH/H_2O_2/H_2O$ (1:1:2). The sacrificial etching mask layer of Cr/Au (35 nm Cr/200 nm Au) was deposited, where Cr served as an adhesive medium between glass and Au. A positive photoresist, S1813, of 1.5 μm thickness was spun on the glass before pattern transfer with Double Side Mask Aligner (MA6/MB6, Karl Suss, Germany). After development in MF-319 for 25 s, exposure and hard-bake at 120 °C for 30 min, Au film was etched with KI/I_2 and Cr film with Cr etchant (KTI Chemicals, Sunnyvale, CA, USA). The HNA solution ($HF/HNO_3/CH_3COOH$: 1:2:1, v/v) was used to engrave the pattern. The channel depth might be periodically checked with Alphastep profilometer (Tencor Ind., San Jose, CA, USA) to establish basic data for future study. The effective separation channel was 5 cm long, 30 μm wide and 10 μm deep, with injection channel crossed at 500 μm from

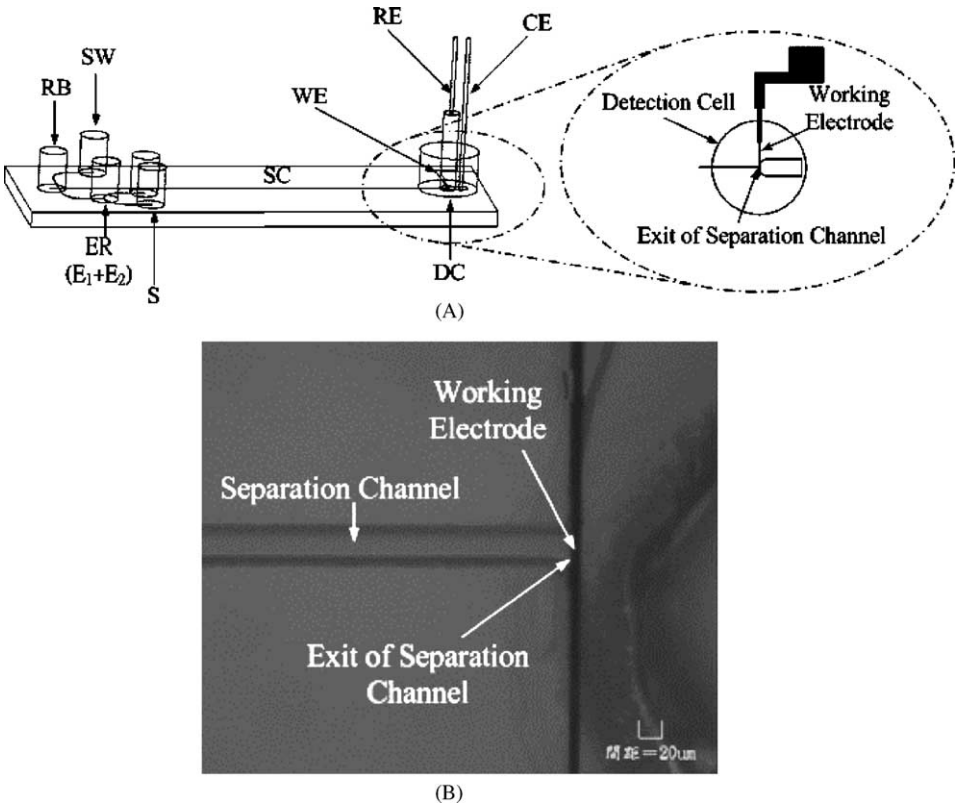

Fig. 1. (A) Schematic layout: running buffer reservoir (RB); sample reservoir (S); enzymatic reaction reservoir (ER ($E_1 + E_2$)); sample waste reservoir (SW); injection channel (ER–SW); separation channel (SC); detection cell (DC); working electrode (WE); reference electrode (RE) and counter electrode (CE). (B) Photograph showing electrode alignment in a completed microchip.

the running buffer reservoir. The injection volume of 6.75 pL was estimated from the 10 μm deep trapezoid formed by the 30 μm top square and the 15 μm bottom square at the cross. Channels between the reservoirs and the flow channels were bored by electric discharge. After duly cleansed, both glass plates were pressed under the load of piled weights in a furnace (Model 2-525 by J. M. Ney Co., Yucaipa, CA) programmed to 650 °C at 3.4 °C min^{-1} before annealed to ambience. Insufficient bonding, almost a definite cause of failing chip, may be spotted by the presence of rainbow. The glass tubing (0.4 cm i.d.) was glued to each hole with epoxy.

2.5. Electrophoresis procedure

After vacuum-flushed with 0.1 M sodium hydroxide, 0.1 M hydrochloric acid and deionized water—each for 10 min—the channels were then flushed with 20 mM phosphate buffer (pH 7.5) for 5 min and rested for 15 min. Sample loading was carried out in two steps. First, the injection channel was filled with the sample solution. A separation potential of +1.5 kV was then applied across the buffer reservoir and the grounded detection reservoir. After baseline stabilized, a potential of +1.5 kV was applied across the sample reservoir and the grounded enzyme reservoir for 5 s to mix the sample and the enzymes in order to ready the reaction product for injection.

2.6. Amperometric detection

Three-electrode configuration, 10 μm Pt film working electrode at +1.0 V against the reference of Ag/AgCl and Pt auxiliary electrode, was employed for all experiments. Amperometric detection was performed with an Electrochemical Analyzer 812 (CH Instruments, Austin, TX, USA), which was connected to a personal computer (Pentium 166 MHz, 32 MB RAM).

3. Results and discussion

3.1. Evaluation of the electrochemical response in the microchannel chip

The embedded microelectrode in a μCE largely meets what an ideal electrochemical detector calls for—sensitivity, responsiveness, durability, and negligible band broadening. However, the troublesome field-induced noises—presumably related to indiscriminate electrode positioning

or improper detector configuration—constantly haunted the workers [9,26,28–30]. It degenerated sensitivity and spoiled the detection level to mMs from the low μMs. The literature had described three primary electrode configurations for μCE; the end-channel, in-channel, and off-channel arrangements [10]. While each configured with respective consideration to boost the detection current, few had done it with grace. The in-channel approach needed a potentiostat in isolation from the high field along with micromaneuvering of the electrode. The requirements were rather difficult to meet, but the peaks were otherwise symmetrical. The off-channel approach suffered from inadequate sensitivity, even if immune from noises. The end-channel design, as shown in Fig. 1A and B, required no more than proximating the electrode to the exit and yet harnessed detection current more effectively. However, the microscopic operation couldn't be exact even with a very fine visual microscope—a few tens of microns off the position could lead to significant peak broadening and sensitivity loss. Painstaking micropositioning pays if sensitivity is a great concern. In this study, the electrode was placed by chance at four microns from the exit. Fig. 2 exemplifies the performance of such configuration; a mixed standard of 100 μM dopamine and 100 μM catechol was drawn into the sample channel by high voltage. Injection was repeatable with controlled injection time. Two resolved peaks eluted in 60 s with N number reaching 26 000 plate m^{-1} for dopamine and 42 000 plate m^{-1} catechol. The R.S.D. ($n = 7$) in migration time for dopamine and catechol were better than 0.35%, while those of peak currents ranged between 4.04 and 5.41%. The calibration curve for dopamine was linear over the range from 0.5 to 1000 μM and catechol from 1 to 1000 μM, with R^2 better than 0.998. The limit of detection, S/N = 3, was 250 nM for dopamine and 500 nM for catechol.

3.2. Precolumn enzymatic reaction

Although anchoring active label has been a ready solution to the problem of inert electroactivity in some bio-important substances, yet the choice between precolumn and postcolumn derivatizations is by no means arbitrary. The old wisdom in conventional CE and HPLC helps; postcolumn derivation is preferred if derivation results in multiple reaction products or unstable ones. However, the demand for fast reaction by fast emergent peaks as such in μCE disqualified it from the list. With separation time as short as a few seconds in μCE, slow derivation dampens response to spoil the peak fidelity.

On the other hand, the precolumn approach with ample time for reaction before injection was free from such concern. The sample reacted with enzyme to liberate hydrogen peroxide together with the reduced mediator NADH; both were eventually separated from ascorbic acid and uric acid. Electropherograms for renal markers and glucose were used for peak identification, as shown in Fig. 3.

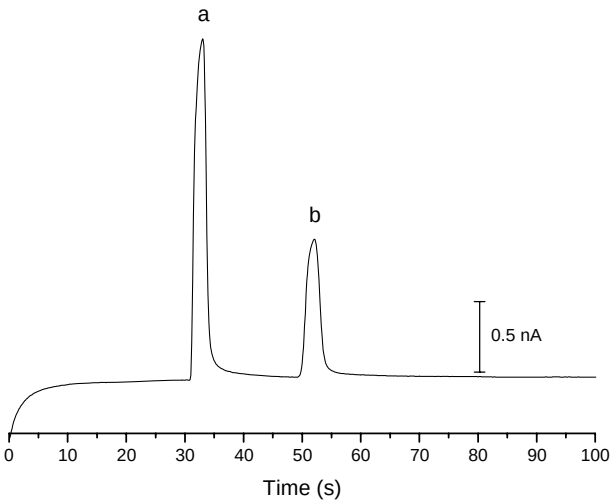

Fig. 2. Electrophoretic separation of (a) dopamine and (b) catechol on CE microchip with amperometric detection. Condition: dopamine and catechol (100 μM); running buffer (25 mM); MES buffer (pH 6.5); separation potential (+1.0 kV); sample loading by applying +1.0 kV across the sample reservoir and the grounded sample waste reservoir for 3 s; amperometric detection at +0.8 V vs. Ag/AgCl at 10 μm Pt film electrode.

Fig. 4 showed the concentration effect of creatininase (A), creatinase (B), sarcosine oxidase (C), and dehydrogenase (D) upon the detector response. Creatinine was converted to H_2O_2 by three consecutive enzymatic reactions [17], and glucose to the electroactive NADH by dehydrogenase. The optimal enzyme concentrations were: 60 U mL^{-1} CA, 43 U mL^{-1} CI, 108 U mL^{-1} SOx and 30 U mL^{-1} GDH. The detection limit of 1 μM was significantly lower than the documented 20 μM [13].

3.3. Selection of working potentials

The working electrode, though employing the end-channel approach with minimized noise from high field [30], a small potential shift was inevitable. The optimal in situ potential was scouted by hydrodynamic voltametry from +0.4 to +1.1 V. The result from a standard solution of uric acid, ascorbic acid, creatinine and glucose is shown in Fig. 5. All, except creatinine, responded to the elevation of working voltage with current gain until upset by the baseline rise beyond +1.0 V.

3.4. Effect of pH and concentration of running buffer

In Fig. 6A, all peaks merged at acidic pH's but gradually resolved beyond pH > 7.5. At pH 7.5, the buffer concentration was optimized at 20 mM, as shown in Fig. 6B.

3.5. Effect of separation voltage and injection time

Increase of separation voltage promoted migration but at the price of noisy signal, as seen in Fig. 6C. The selection of

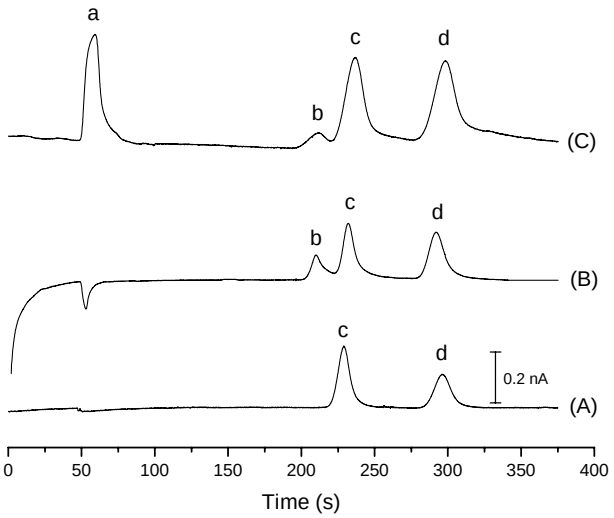

Fig. 3. Electropherograms for (A) a mixture containing 200 μM ascorbic acid (c) and 200 μM uric acid (d); (B) a mixture containing 200 μM glucose (b), 200 μM ascorbic acid (c) and 200 μM uric acid (d); (C) a mixture containing 250 μM creatinine (a), glucose (b), ascorbic acid (c) and uric acid (d). Conditions: separation voltage at +1.5 kV; electrokinetic injection for 5 s (at +1.5 kV); working potential, +1.0 V (vs. Ag/AgCl) at 10 μm Pt film electrode; running buffer of 20 mM; phosphate buffer (pH 7.5). Reagent solution: CA (60 U mL^{-1}); CI (43 U mL^{-1}); SOx (108 U mL^{-1}); GDH (30 U mL^{-1}) and NAD$^+$ (20 mM).

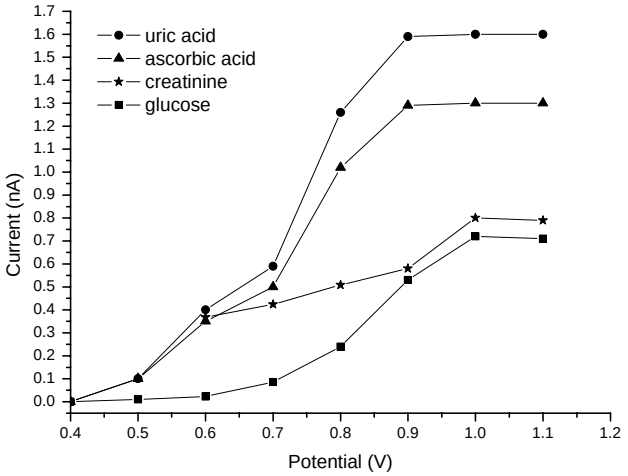

Fig. 5. Hydrodynamic voltammograms (HDVs) for 200 μM of uric acid, ascorbic acid, creatinine, and glucose. Conditions: separation voltage at +1.5 kV; electrokinetic injection for 5 s (at +1.5 kV); working electrode with 10 μm Pt film electrode; running buffer of 20 mM; phosphate buffer (pH 7.5). Reagent solution: CA (60 U mL^{-1}); CI (43 U mL^{-1}); SOx (108 U mL^{-1}); GDH (30 U mL^{-1}); NAD$^+$ (20 mM).

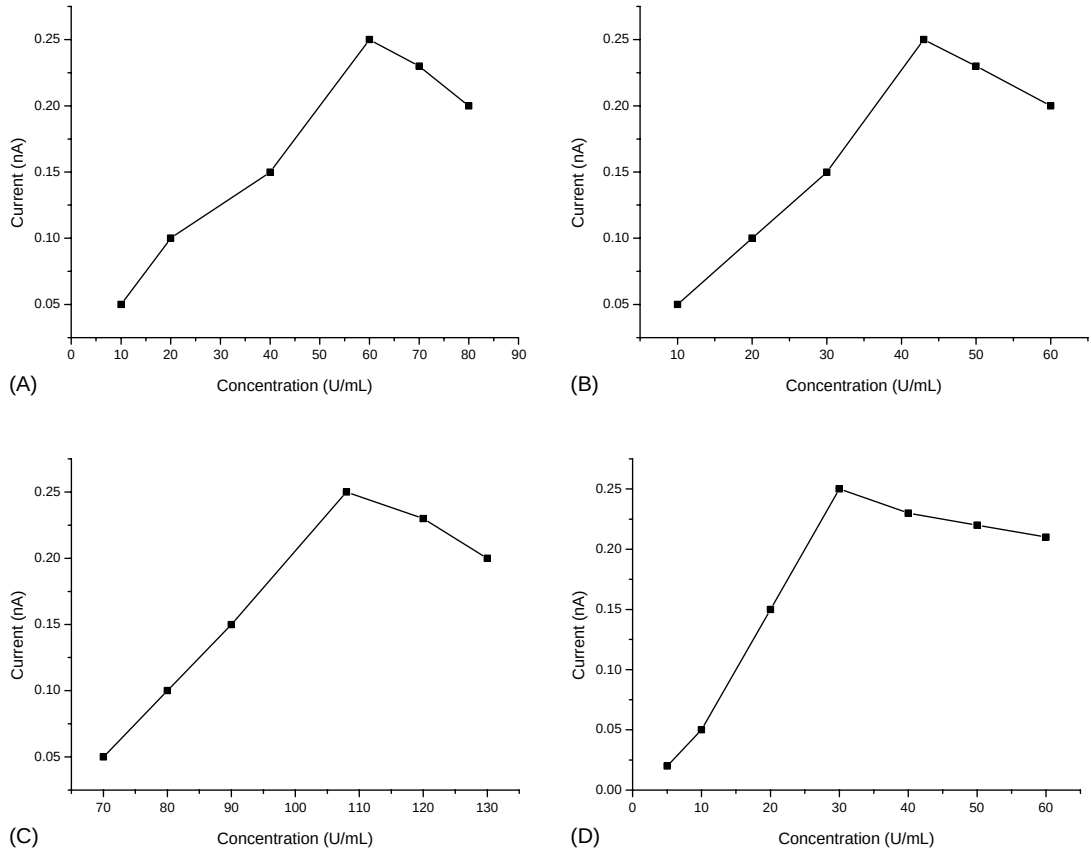

Fig. 4. Effect of the CA (A), CI (B), SOx (C) and GDH (D) level on the response of 250 μM creatinine, glucose, ascorbic acid and uric acid (other conditions, as in Fig. 3).

1.5 kV was a trade-off between the two. Prolonging injection time would accommodate more samples via dispersion at the intersection. However, oversized sample from prolonging beyond 5 s would lead to broadened peaks, as shown in Fig. 6D. The current–reaction-time curve leveled off after 5 s, as shown in 6E.

3.6. Reproducibility, linearity and detection limits of the analytes

The migration time was repeatable from injection to injection, better than 0.5% R.S.D. ($n = 7$), for all four compounds. The range of variation in peak current was between

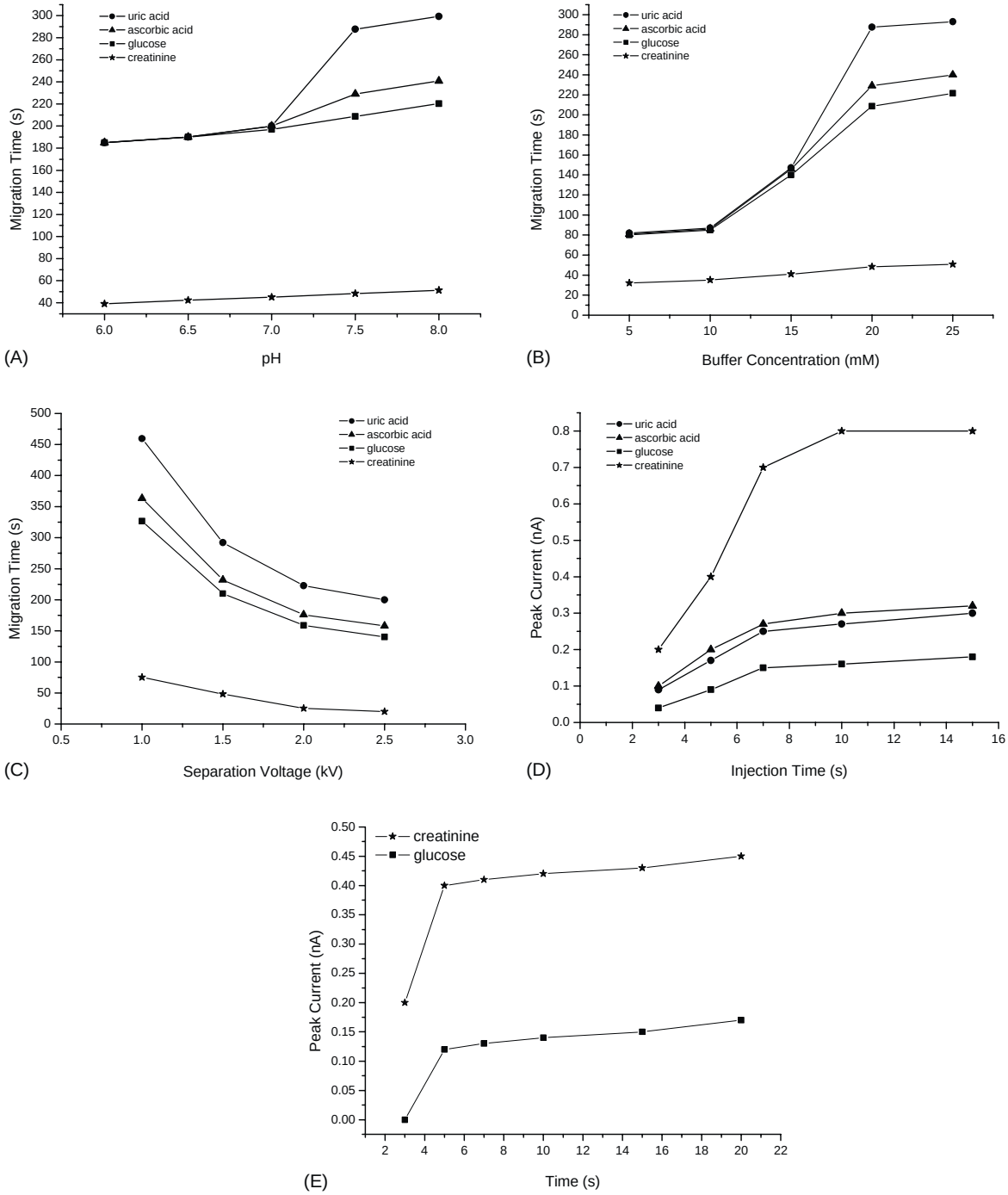

Fig. 6. Effect of (A) acidity and (B) concentration of running buffer, (C) separation voltage on migration time, (D) effect of injection time on peak current and (E) effect of reaction time on peak current. Working potential: +1.0 V (vs. Ag/AgCl) at the 10 μm Pt film electrode; electrokinetic injection for 5 s (at +1.5 kV). Reagent solution: CA (60 U mL^{-1}); CI (43 U mL^{-1}); SOx (108 U mL^{-1}); GDH (30 U mL^{-1}); NAD$^+$ (20 mM).

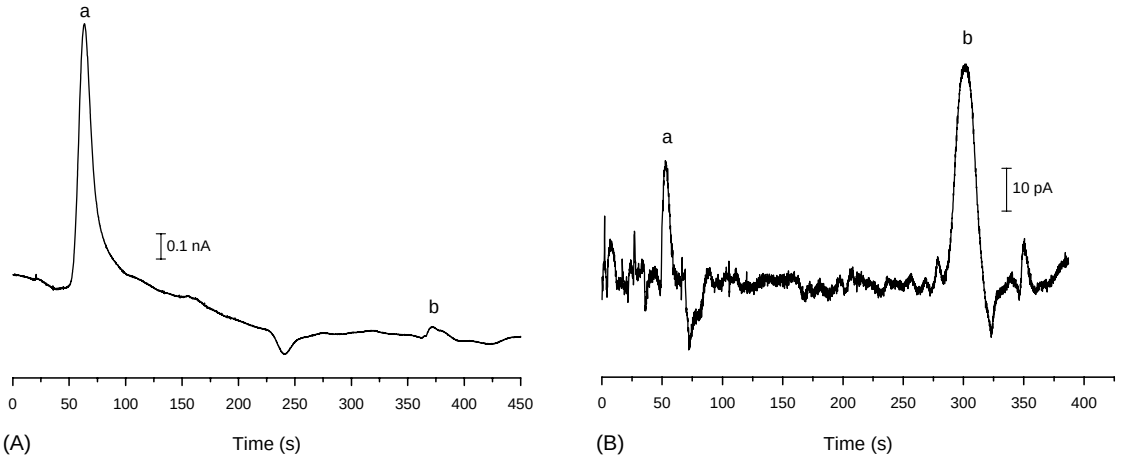

Fig. 7. Electropherograms of (A) a 10-fold dilution of human urine sample and (B) human serum: (a) creatinine and (b) uric acid. Conditions: separation voltage at +1.5 kV; electrokinetic injection for 5 s (at +1.5 kV); working potential, +1.0 V (vs. Ag/AgCl) at 10 μm Pt film electrode; running buffer of 20 mM phosphate buffer (pH 7.5). Reagent solution: CA (60 U mL^{-1}); CI (43 U mL^{-1}); SOx (108 U mL^{-1}).

Table 1
The regression equation and detection limit[a]

Analyte	Regression equation $y = bx^{b} + a$	Correlation coefficient	Linear range (μM)	Detection limit[c] (μM)
Creatinine	$y = 0.730x + 0.020$	0.9952	10–600	1
Glucose	$y = 1.306x - 0.002$	0.9955	10–800	10
Ascorbic acid	$y = 18.91x - 0.264$	0.9983	10–600	0.71
Uric acid	$y = 18.82x + 0.005$	0.9987	10–800	2.3

[a] Detection potential is +1.0 V against Ag/AgCl. Other conditions as in Fig. 3.
[b] y and x are the peak current (nA) and concentration of the analytes (mM), respectively.
[c] Detection limits were based on the signal-to-noise ratio of 3.

1.5 and 2.2%. The calibration curves were linear from 10 to 800 μM, with $R^2 > 0.995$. The results were tabulated in Table 1. The detection limit of ascorbic acid, S/N = 3, was 0.71 μM, but glucose 10 μM.

3.7. Analytical applications

Urine and serum samples were assayed to demonstrate the application potential of the present microchip for use as high-throughput clinical tool. Urine samples were diluted 10-fold and filtered before injection, while serum samples were injected as received before filtration. Creatinine and uric acid were separated in 400 s, as shown in Fig. 7A and B. The urine sample ($n = 3$) consisted of 14 mM creatinine and 23 μM uric acid, with serum 5.5 and 2.1 μM.

4. Conclusions

We have demonstrated a biochip employing the end-channel electrode and precolumn enzymatic reactions for the analysis of renal markers of creatinine and uric acid, and glucose. Its economy, speed, sensitivity and separation efficiency would qualify itself for point-of-care needs in medical diagnosis and food industries. This is especially true with an embedded electrode design which benefits fabrication.

In the strategy of using multiple enzymes, though not entirely new, none had used the more reliable approach of precolumn enzyme reactions or succeeded in accommodating more substances in a single run. The former was inherent with stabilized baselines and fast responding peaks, as opposed to those with on-column or post-column one. The latter was important in diagnosing kidney problems for the long-time sufferers of diabetes. More importantly, it could lead to high-throughput clinical diagnostic tools if incorporating parallel channels.

Acknowledgements

The authors thank the National Science Council (Grant no. NSC91-2113-M-030-010) for financial support, and Northern Region MEMS Research Center (Taipei) of the National Science Council of the Republic China for facilities to support the MEMS fabrication.

References

[1] A. Manz, D.J. Harrison, E.M.J. Verpoorte, J.C. Fettinger, A. Paulus, H. Ludi, H.M. Widmer, J. Chromatogr. 593 (1992) 253.

[2] C.S. Effenhauser, A. Manz, H.M. Widmer, Anal. Chem. 65 (1993) 2637.
[3] C.L. Colyer, T. Tang, N. Chiem, D.J. Harrison, Electrophoresis 18 (1997) 1733.
[4] D. Figeys, D. Pinto, Electrophoresis 22 (2001) 208.
[5] J. Wang, Electrophoresis 23 (2002) 713.
[6] A.G. Hadd, S.C. Jacobson, J.M. Ramsey, Anal. Chem. 71 (1999) 2637.
[7] A.G. Hadd, D. Raymond, J. Halliwell, S.C. Jacobson, J.M. Ramsey, Anal. Chem. 69 (1997) 3407.
[8] S.A. Zugel, B. Burke, F. Regnier, F.E. Lytle, Anal. Chem. 72 (2000) 5731.
[9] J. Wang, Talanta 56 (2002) 223.
[10] W.R. Vandaveer IV, S.A. Pasas, R.S. Martin, S.M. Lunte, Electrophoresis 23 (2002) 3667.
[11] J. Wang, M.P. Chatrathi, B. Tian, Anal. Chem. 73 (2001) 1296.
[12] J. Wang, M.P. Chatrathi, B. Tian, R. Polsky, Anal. Chem. 72 (2000) 2514.
[13] J. Wang, M.P. Chatrathi, Anal. Chem. 75 (2003) 525.
[14] J. Wang, M.P. Chatrathi, A. Ibáñez, A. Escarpa, Electroanalysis 14 (2002) 400.
[15] J. Wang, A. Ibáñez, M.P. Chatrathi, A. Escarpa, Anal. Chem. 73 (2001) 5323.
[16] J. Clark, The Kidneys Balancing the Fluids, Torstar Books, New York, 1985.
[17] J. Delanghe, M.D. Buyzere, I.D. Scheerder, D. Vogelaers, J. Van den Bogaerde, A.M. Van den Abeele, P. Gheeraert, R. Wieme, Ann. Clin. Biochem. 25 (1988) 383.
[18] C.A. Burtis, E.R. Ashwood, Tietz Fundamentals of Clinical Chemistry, Saunders, Philadelphia, 1996, p. 569.
[19] H.W. Smith, The Kidney Structure and Function in Health and Disease, Oxford University Press, New York, 1951.
[20] J. Wang, Electroanalysis 13 (2001) 983.
[21] T. Tsuchida, K. Yoda, Clin. Chem. 29 (1983) 51.
[22] R. Kock, B. Sitz, B. Delvoux, H. Greiling, Eur. J. Clin. Chem. Biochem. 33 (1995) 23.
[23] N.D. Burke, H.C. Sing, W.E. Neeley, S.E. Koetitz, Clin. Chem. 23 (1977) 1281.
[24] E.A. Clark, J.C. Fanguy, C.S. Henry, J. Parm. Biomed. Anal. 25 (2001) 795.
[25] J.C. Jaffe, Hoppe-Seyler's. Z. Physiol. Chem. 10 (1886) 391.
[26] A.T. Woolley, K.Q. Lao, A.N. Galazer, R.A. Mathies, Anal. Chem. 70 (1998) 684.
[27] G.T.A. Kovacs, Micromachined Transducers Sourcebook, McGraw-Hill, New York, 1998, p. 98.
[28] R.S. Martin, K.L. Ratzlaff, B.H. Huynh, S.M. Lunte, Anal. Chem. 74 (2002) 1136.
[29] J.A. Lapos, D.P. Manica, A.G. Ewing, Anal. Chem. 74 (2002) 3348.
[30] O. Klett, F. Bjorefors, L. Nyholm, Anal. Chem. 73 (2001) 1909.